4-23-2013

A High Energy Density All Solid-State Tungsten-Air Battery

Xuan Zhao
University of South Carolina - Columbia, zhao53@email.sc.edu

Xue Li
University of South Carolina - Columbia, lixue@cec.sc.edu

Yunhui Gong

Nansheng Xu
University of South Carolina - Columbia, xun@cec.sc.edu

Kevin Gregory Romito
University of South Carolina, romito@email.sc.edu

See next page for additional authors

Publication Info

Published in *Chemical Communications*, Volume 49, Issue 47, 2013, pages 5357-5359.

This article was first published by the Royal Society of Chemistry and can be found at http://dx.doi.org/10.1039/C3CC42075B
Zhao, X., Li, X., Gong, Y., Xu, N., Romito, K., & Huang, K. (2013). A High Energy Density All Solid-State Tungsten-Air Battery. Chemical Communications, 49 (47), 5357 - 5359. http://dx.doi.org/10.1039/C3CC42075B

Author(s)
Xuan Zhao, Xue Li, Yunhui Gong, Nansheng Xu, Kevin Gregory Romito, and Kevin Huang

All Solid-State Tungsten-Air Battery

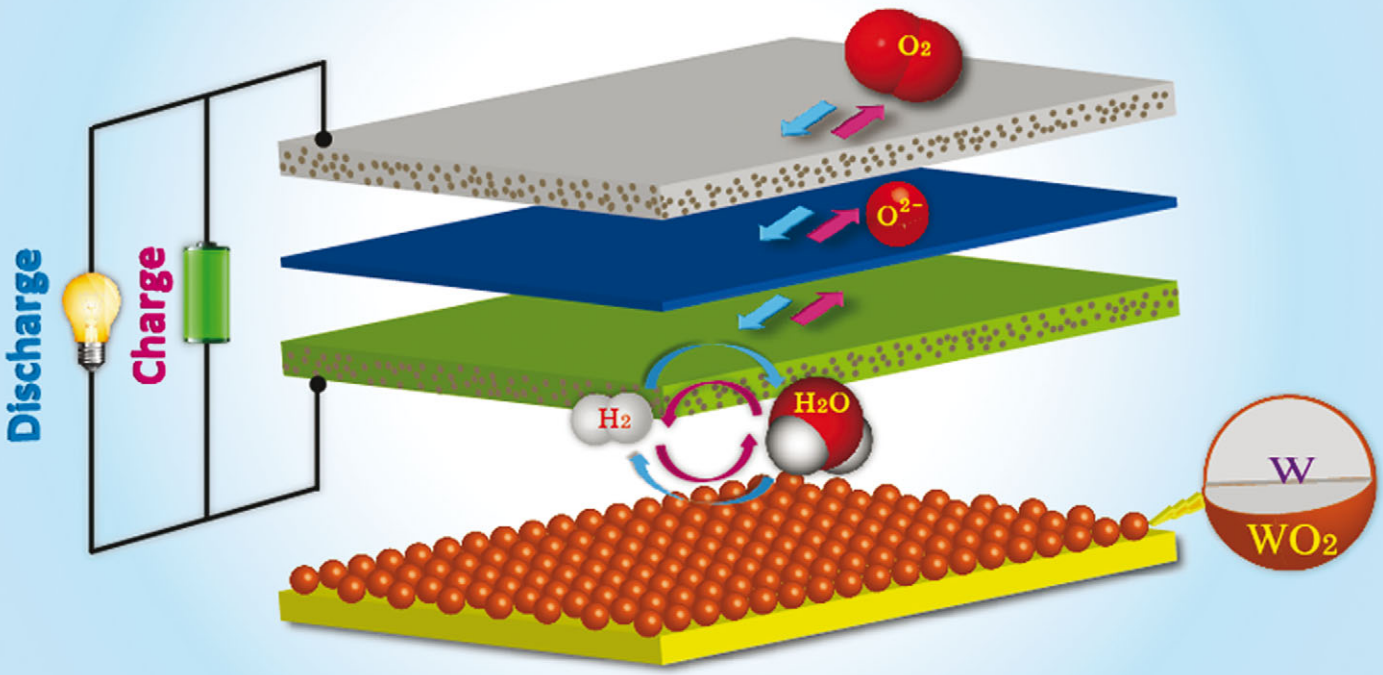

Showcasing research from Dr. Kevin Huang's Laboratory, Department of Mechanical Engineering, University of South Carolina, Columbia, SC, USA

A high energy density all solid-state tungsten–air battery

An all solid-state tungsten–air battery using solid oxide–ion electrolyte is demonstrated as a new chemistry for advanced energy storage. The unique design of separated energy storage from the electrodes allows for free volume expansion–contraction during electrical cycles and new metal–air chemistry to be explored conveniently.

As featured in:

See Kevin Huang *et al.*, *Chem. Commun.*, 2013, **49**, 5357.

RSC Publishing

www.rsc.org/chemcomm

Registered Charity Number 207890

ChemComm

RSC Publishing

COMMUNICATION

View Article Online
View Journal | View Issue

A high energy density all solid-state tungsten–air battery†

Cite this: *Chem. Commun.*, 2013, **49**, 5357

Received 21st March 2013,
Accepted 22nd April 2013

DOI: 10.1039/c3cc42075b

www.rsc.org/chemcomm

Xuan Zhao, Xue Li, Yunhui Gong, Nansheng Xu, Kevin Romito and Kevin Huang*

An all solid-state tungsten–air battery is reported here, which is based on a new metal–air chemistry, featuring decoupled design of electrodes and energy storage. Benefited from higher specific density and better redox kinetics of tungsten, the new tungsten–air battery exhibits roughly higher energy density (W h L^{-1}) than the previously reported iron–air battery.

Rechargeable batteries represent an advanced class of electrochemical energy storage devices that can find a broad application in small-scale portable consumer electronics, mid-scale electrical vehicles and large-scale electric grids. An emerging branch of rechargeable batteries is based on the metal–air chemistry, featuring extremely high specific energy (W h kg^{-1})/energy density (W h L^{-1}) and inexhaustible and storage-free cathode reactants.[1–11] However, key issues limiting the commercial development of the conventional metal–air batteries (*e.g.*, lithium–air, iron–air and zinc–air) for mid-scale transportation and large-scale stationary applications are the poor reversibility and low rate capacity arising from technical issues such as congestion of air-pathways by the formation of condensed oxides,[6] precipitation of carbonates in electro-catalyst's pores in the air-electrode,[7,8] and evaporation/decomposition of liquid organic solvent electrolytes.[7,9–11]

Recently, we demonstrated a novel concept of the "all solid-state metal–air battery" that innovatively combines a regenerative solid oxide fuel cell (or RSOFC) and a chemical-looping redox cycle unit (RCU).[12,13] The air-electrode reactions in this battery involve only reduction and evolution of gaseous O_2, making clogging of the air-pathway no longer an issue. In addition, solid oxide-ion electrolytes are known to be stable in a broad range of gas mixtures and in contact with a variety of oxides. Therefore, the new battery is expected to be free of the aforementioned reactivity problems for the conventional liquid-electrolyte based "metal–air" batteries.

In the new battery, the RSOFC serves as the "electrical functioning unit" operating alternately between the fuel cell and electrolyzer modes to realize the discharge and charge cycles, while the RCU acts as the "energy storage unit (ESU)" to carry out reversible chemical–electrical energy conversion *in situ via* H_2–H_2O-mediated metal/metal-oxide (Me/MeO_x) redox reactions. The distinct advantages of this innovative battery design over conventional metal–air batteries include double electron-transfer (O^{2-}), state-of-charge independent EMF (electromotive force), high specific energy and energy density, and independent design of power and energy.[12,13] More appealingly, the new battery stores chemical energy in redox couples that are physically separated from electrodes of RSOFC as illustrated in Fig. 1, avoiding the shape change problem of conventional chemical batteries. For more experimental details and characterization of the battery, refer to the ESI.†

The unique design of decoupled electrodes and energy storage allows for exploitation of other metal–air chemistries by simply changing the redox couple in the ESU. Here, we report for the first time on an all solid-state rechargeable tungsten–air battery using W–WO_2 as the redox-couple. The selection of W–WO_2 redox couple as the ESU is rationalized by its favourable thermodynamic and kinetic properties shown in Fig. 2 and 3. From the phase diagram shown in Fig. S1 (ESI†), it is found that W and WO_2 are the two equilibrium phases within the temperature range of interest, thus constituting a stable redox couple for the battery.

The working principle of the all solid-state tungsten–air battery using H_2–H_2O as the mediation gas to facilitate the metal/metal-oxide redox reaction is schematically shown in Fig. 1, using a planar cell geometry.

The operation of a charge and discharge cycle can be described as follows. During the discharge, the interaction between

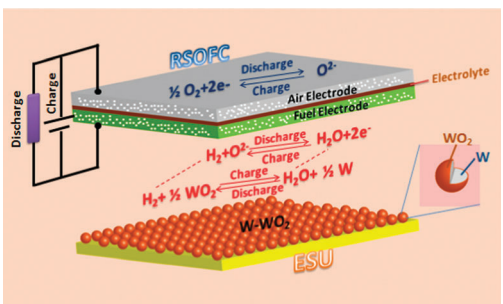

Fig. 1 A schematic illustration of the working principle of the new rechargeable all solid-state tungsten–air battery.

Department of Mechanical Engineering, University of South Carolina, Columbia, SC29201, USA. E-mail: kevin.huang@sc.edu; Fax: +1 803 777 0106; Tel: +1 803 777 4185

† Electronic supplementary information (ESI) available: Experimental details and maximum charge density. See DOI: 10.1039/c3cc42075b

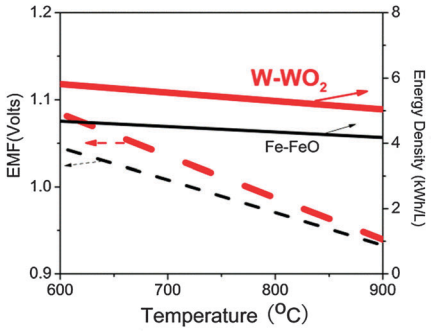

Fig. 2 Comparison of EMF and theoretical energy density between W–WO_2 and Fe–FeO redox couples as a function of temperature. The calculation is based on molar volume of metal oxide.

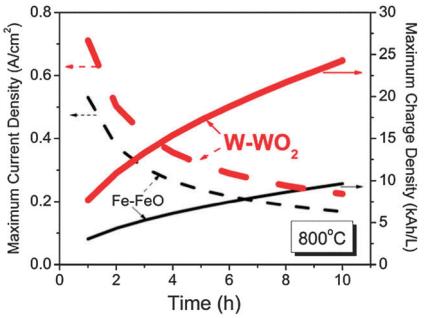

Fig. 3 Comparison of maximum charge density of ESU and maximum current density of RSOFC matched with the kinetics of redox reactions at 800 °C. (Note: $(S_{ESU}m_{ESU})/A_{RSOFC}$ = 10/1 as a realistic ratio is assumed in the calculation.)

H_2O and W produces H_2 locally in the ESU *via* the following chemical reaction

$$W_{(s)} + 2H_2O_{(g)} = WO_{2(s)} + 2H_{2(g)} \quad (1)$$

The generated H_2 then diffuses to the fuel-electrode surface of the RSOEC operating in fuel-cell mode by which H_2 is electrochemically oxidized, producing electricity and H_2O *via* the following electrochemical reaction

$$H_{2(g)} + O^{2-} = H_2O_{(g)} + 2e^- \quad (2)$$

The product H_2O then diffuses back to the surface of W and further reacts to produce more H_2 to keep reaction (1) active. When all (or a controlled portion of) the W phase is oxidized and no (or a controlled portion of) H_2 is produced, the discharge cycle is stopped and the battery needs to be recharged. For the charge cycle, the H_2O in the mediation gas, H_2–H_2O, is electrochemically split into H_2 at the fuel-electrode of the RSOFC operating in the electrolysis mode

$$H_2O_{(g)} + 2e^- = H_{2(g)} + O^{2-} \quad (3)$$

The generated H_2 then migrates to the ESU where WO_2 is chemically reduced to W as

$$WO_{2(s)} + 2H_{2(g)} = W_{(s)} + 2H_2O_{(g)} \quad (4)$$

The product H_2O is then further split as in reaction (3) to produce more H_2 for reaction (4). When all (or a controlled portion of) WO_2 is reduced to W by H_2 and no (or a controlled portion of) H_2O is produced, the charge cycle is completed. The freshly reduced and chemically active W is then ready for the next discharge cycle as described by reactions (1) and (2). According to the Gibbs phase rule, the residual freedom $F_r = 0$ for a dual-phase (P = 2) binary system (C = 2) under isothermal and isobaric conditions, which implies that the intensive quantity electrode potential is independent of the state-of-charge.

The overall chemical reaction summarized from individual reactions (1)–(4) occurring inside the battery can be written as

$$W_{(s)} + O_{2(g)} = WO_{2(s)} \quad (5)$$

The rationale for choosing the W–WO_2 redox couple as the ESU is two-fold. First, the maximum theoretical specific energy (MTSE, W h kg^{-1}) of the all solid-state metal–air battery depends on the number of electrons involved in the redox reaction and the mass loading of the active metal in a battery. For a battery with a finite volume, denser metals with more oxygen per unit formula of oxides would allow more mass loading and higher oxygen storage capacity per unit volume, and thus more energy capacity could be stored. Tungsten is a heavy metal with a specific density of 19.25 g cm^{-3}. Its equilibrium oxide WO_2 contains 2 O per unit formula. Therefore, as an active metal it has the advantage of achieving higher energy density (W h L^{-1}). Thermodynamic analysis shown in Fig. 2 indeed suggests that the W–WO_2 redox-couple has an appreciably higher theoretical energy density than Fe–FeO. In addition, the W–WO_2 couple also has a marginal EMF advantage over Fe–FeO.

Second, the cycle efficiency (or round-trip efficiency) as well as the cycle stability depend on the reversibility of the redox reactions in the ESU. The maximum charge density of ESU (Q_{max}, kA h L^{-1}) of redox couples and the corresponding maximum current density of RSOFC (J_{max}, A cm^{-2}) are the two important properties of the battery. They represent the upper limits to the charge and energy capacities achievable by the battery. The premise for calculating Q_{max} and J_{max} is that the rate of charge-transfer (current) of RSOFC must match the rate of the redox reactions in order to sustain the battery's functionality. The deduction of Q_{max} and J_{max} equations starts from the parabolic kinetics governing the redox reaction:

$$(\Delta m)^2 = K_p t \quad (6)$$

here Δm is the mass change of the sample, g cm^{-2}; K_p is the parabolic rate constant of redox kinetics, g^2 cm^{-4} s^{-1}; t is the time, s. Combining eqn (6) with Faraday's law yields the maximum charge density Q_{max} (kA h L^{-1}) of the battery:

$$Q_{max} = \frac{\Delta m S_{ESU}}{M_O \times 3600} \times 2Fx \times \rho \quad (7)$$

where M_O is the atomic weight of oxygen, 16 g mol^{-1}; x is the oxygen stoichiometry of MeO_x; S_{ESU} is the specific surface area of the redox materials in ESU, cm^2 g^{-1}; ρ is the density of the redox materials in ESU, g cm^{-3}. Substituting eqn (6) into eqn (7) leads to the maximum charge density:

$$Q_{max} = \frac{2Fx \times \rho\sqrt{K_p t}}{M_O \times 3600} \times S_{ESU} \quad (8)$$

The equivalent maximum current density, J_{max} (A cm^{-2}), of RSOFC is then given as

$$J_{max} = \frac{3600Q_{max}}{tA_{RSOFC}} \times \frac{m_{ESU}}{\rho} = \frac{2Fx \times \sqrt{K_p/t}}{M_O A_{RSOFC}} \times (S_{ESU} m_{ESU}) \quad (9)$$

where m_{ESU} is the mass loading of the redox material in ESU; A_{RSOFC} is the active electrode area of RSOFC. Due to the scarcity of kinetic rate constants related to metal oxidation/reduction in the H_2O–H_2 mixture, K_p values obtained from experiments conducted in air were used for the sake of comparison.[14,15] The rate of metal oxidation in steam is expected to be faster than that in air because the former has a faster surface reaction and produces a relatively more porous scale than the latter.[16] Therefore, the use of air-derived K_p values for the calculation is deemed relatively conservative.

Fig. 3 compares Q_{max} and J_{max} of W–WO_2 and Fe–FeO calculated as a function of cycle duration. It is evident that W–WO_2 is kinetically more favourable than Fe–FeO. It should be noted that the relative mass (therefore volume) between metal and metal-oxide phases in the redox couple varies with the state-of-charge. To be conservative, we chose the specific density ρ of WO_2 (10.8 g cm^{-3}) instead of W (19.25 g cm^{-3}) in the calculation. The readers can also see the difference in metal-based calculation in the ESI.†

The energy storage characteristics of the all solid-state tungsten–air battery obtained at 800 °C are shown in Fig. 4(a). Refer to the ESI† for experimental details. The battery was continuously cycled at J = 100 mA cm^{-2} for three consecutive 2 hour cycles, producing a discharge charge-density of 5.36 kA h L^{-1} and a discharge energy-density of 3.55 kW h L^{-1} with a round-trip efficiency of 53%. The operating current density J = 100 mA cm^{-2} is well below J_{max} = 500 mA cm^{-2} of W–WO_2 shown in Fig. 3 for a 2 h cycle, which ensures that the rate of redox kinetics is fast enough to sustain the battery's current density. Similarly, the iron–air battery with the same ESU-volume was cycled under the same conditions, but producing a lower discharge charge-density of 4.45 kA h L^{-1}, discharge energy-density of 2.90 kW h L^{-1}, and round trip efficiency of 50% than the tungsten–air battery, see Fig. 4(b). The roughly 22% higher energy-density of the W–air battery than the Fe–air one is evidently the result of the higher specific density of tungsten considering the fact that the W–air battery in fact exhibits a lower operating voltage than the Fe–air battery. The slightly higher round-trip efficiency of the tungsten–air battery appears to benefit from faster redox kinetics as suggested in Fig. 3. Note that the energy densities shown in Fig. 4 are normalized to the metal-oxide volume that is equivalent to an oxygen flux needed to sustain the redox reaction. Such normalization allows for comparison with theoretical values such as those shown in Fig. 2. The comparisons clearly indicate that the achieved energy density only represents 67% of the theoretical value, which implies that a portion of energy has been lost to RSOFC polarization reactions and ESU redox kinetic resistances. Therefore, optimization of these components to achieve a better performance at lower temperatures should be a priority for future studies. This is particularly in line with the need to further improve the cycle stability of the new tungsten–air battery, which has not yet been demonstrated in this study.

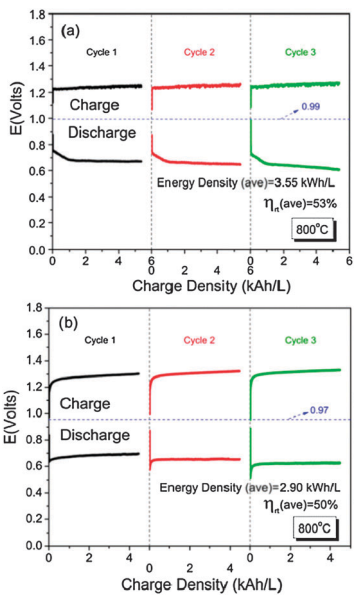

Fig. 4 Battery voltage as a function of charge-density for the all solid-state metal–air battery: (a) tungsten–air; (b) iron–air; operating current density J = 100 mA cm^{-2}.

We have demonstrated proof-of-concept of a new high energy-density all solid-state tungsten–air rechargeable battery in this study. The new battery operates alternately between the fuel cell and electrolysis modes of a regenerative solid oxide fuel cell to realize the discharge and charge cycles, respectively, while *in situ* electrical–chemical energy conversion is achieved through H_2–H_2O-mediated W–WO_2 redox reaction. Within a limited number of cycles tested, the tungsten–air battery exhibits high charge- and energy-density with moderate cycle efficiency. Future research will be focused on improving the cycle efficiency and cycle stability through optimizing the performance of RSOFC and kinetics of W–WO_2. Due to the nature of high specific density of tungsten, the tungsten–air battery is considered more suited for stationary energy storage.

Notes and references

1 Z. Peng, S. A. Freunberger, Y. Chen and P. G. Bruce, *Science*, 2012, **337**, 563.
2 Y. C. Lu, H. A. Gasteiger and Y. Shao, *J. Am. Chem. Soc.*, 2011, **133**, 19048.
3 O. Chusid, Y. Gofer, H. Gizbar, Y. Vestfrid, E. Levi, D. Aurbach and I. Riech, *Adv. Mater.*, 2003, **15**, 627.
4 S. R. Narayanan, G. K. Prakash, A. Manohar, B. Yang, S. Malkhandi and A. Kindler, *Solid State Ionics*, 2012, **216**, 105.
5 K. Takechi, T. Shiga and T. Asaoka, *Chem. Commun.*, 2011, **47**, 3463.
6 Y. Shao, S. Park, J. Xiao, J. Zhang, Y. Wang and J. Liu, *ACS Catal.*, 2012, **2**, 844.
7 B. D. McCloskey, A. Speidel, R. Scheffler, D. C. Miller, V. Viswanathan, J. S. Hummelshoj, B. D. McCloskey, A. Speidel, R. Scheffler, D. C. Miller, V. Viswanathan, J. S. Hummelshøj, J. K. Nørskov and A. C. Luntz, *J. Phys. Chem. Lett.*, 2012, **3**, 997.
8 H. Wang and K. Xie, *Electrochim. Acta*, 2012, **64**, 29.
9 Y. C. Lu, E. J. Crumlin, G. M. Veith, J. R. Harding, E. Mutoro, L. Baggetto, N. J. Dudney, Z. Liu and Y. Shao-Horn, *Sci. Rep.*, 2012, **2**, 715.
10 S. A. Freunberger, Y. Chen, Z. Peng, J. M. Griffin, L. J. Hardwick, F. Bardé, P. Novák and P. G. Bruce, *J. Am. Chem. Soc.*, 2011, **133**, 8040.
11 S. A. Freunberger, Y. Chen, N. E. Drewett, L. J. Hardwick, F. Bardé and P. G. Bruce, *Angew. Chem., Int. Ed.*, 2011, **50**, 8609.
12 N. Xu, X. Li, X. Zhao, J. B. Goodenough and K. Huang, *Energy Environ. Sci.*, 2011, **4**, 4942.
13 X. Zhao, N. Xu, X. Li, Y. Gong and K. Huang, *RSC Adv.*, 2012, **2**, 10163.
14 E. A. Gulbransen and K. F. Andrew, *J. Electrochem. Soc.*, 1960, **107**, 619.
15 V. O. Kubaschewski and B. E. Hopkins, *Oxidation of metals and alloys*, New York, 1953.
16 S. R. J. Suaders, M. Monterio and F. Rizzo, *Prog. Mater. Sci.*, 2008, **53**, 775.